analytical chemistry

Freie Universität Berlin

Subscriber access provided by UB + Fachbibliothek Chemie | (FU-Bibliothekssystem)

Article

Universal Dynamic DNA Assembly-Programmed Surface Hybridization Effect for Single-step, Reusable, and Amplified Electrochemical Nucleic Acid Biosensing

Shufeng Liu, Li Fang, Yanqun Wang, and Li Wang

Anal. Chem., **Just Accepted Manuscript** • DOI: 10.1021/acs.analchem.6b04871 • Publication Date (Web): 03 Feb 2017

Downloaded from http://pubs.acs.org on February 5, 2017

Just Accepted

"Just Accepted" manuscripts have been peer-reviewed and accepted for publication. They are posted online prior to technical editing, formatting for publication and author proofing. The American Chemical Society provides "Just Accepted" as a free service to the research community to expedite the dissemination of scientific material as soon as possible after acceptance. "Just Accepted" manuscripts appear in full in PDF format accompanied by an HTML abstract. "Just Accepted" manuscripts have been fully peer reviewed, but should not be considered the official version of record. They are accessible to all readers and citable by the Digital Object Identifier (DOI®). "Just Accepted" is an optional service offered to authors. Therefore, the "Just Accepted" Web site may not include all articles that will be published in the journal. After a manuscript is technically edited and formatted, it will be removed from the "Just Accepted" Web site and published as an ASAP article. Note that technical editing may introduce minor changes to the manuscript text and/or graphics which could affect content, and all legal disclaimers and ethical guidelines that apply to the journal pertain. ACS cannot be held responsible for errors or consequences arising from the use of information contained in these "Just Accepted" manuscripts.

ACS Publications

Analytical Chemistry is published by the American Chemical Society. 1155 Sixteenth Street N.W., Washington, DC 20036

Published by American Chemical Society. Copyright © American Chemical Society. However, no copyright claim is made to original U.S. Government works, or works produced by employees of any Commonwealth realm Crown government in the course of their duties.

Universal Dynamic DNA Assembly-Programmed Surface Hybridization Effect for Single-step, Reusable, and Amplified Electrochemical Nucleic Acid Biosensing

Shufeng Liu*, Li Fang, Yanqun Wang, and Li Wang

Key Laboratory of Sensor Analysis of Tumor Marker, Ministry of Education, College of Chemistry and Molecular Engineering, Qingdao University of Science and Technology, No.53, Rd. Zhengzhou, Qingdao, Shandong 266042, China.

*Corresponding author. Tel.&Fax. 86-532-84022681. E-mail address: sliu@qust.edu.cn

ABSTRACT

The traditional sensitive electrochemical biosensors are commonly confronted with the cumbersome interface operation and washing procedures and/or the inclusion of extra exogenous reagents, which impose the challenge on the detection simplicity, reliability and reusability. Herein, we present the proof-of-principle of a unique biosensor architecture based on dynamic DNA assembly-programmed surface hybridization, which confers the single-step, reusable and enzyme-free amplified electrochemical nucleic acid analysis. To demonstrate the fabrication universality three dynamic DNA assembly strategies including DNA-fueled target recycling, catalytic hairpin DNA assembly and hybridization chain reaction were flexibly harnessed to convey the homogenous target recognition and amplification events into various DNA scaffolds for the autonomous proximity-based surface hybridization. The current biosensor architecture features generalizability, simplicity, low cost, high sensitivity and specificity over the traditional nucleic acid-related amplified biosensors. The lowest detection limit of 50 aM toward target DNA could be achieved by hybridization chain reaction-programmed surface hybridization. The reliable working ability for both homogenous solution and heterogenous inteface facilitates the target analysis with a robust reliability and reproducibility, also making it to be readily extended for the integration with the kinds of detecting platforms. Thus it may hold great potential for the biosensor fabrication served for the point-of-care applications in resource constrained regions.

Keywords: Dynamic DNA assembly; Electrochemical biosensor; Nucleic acid; Target recycling; Hybridization chain reaction

INTRODUCTION

During the past decades, the development of amplified nucleic acid biosensors has drawn gradual attentions for the applications in molecular recognition, medical diagnosis and environmental monitoring.[1-4] The electrochemical detection features prominently because it confers great signal stability, simple instrumentation and ease of calibration.[5-7] To fulfill the demands for the profiling of trace amounts of nucleic acid, the combination of signal amplification step during the biosensor fabrication process is almost an inevitable option.[8-10] However, the relatively complex interface operation and washing procedures and/or the inclusion of extra exogenous reagents for the most available heterogenous biosensors not only increase the assay time and cost, but also would not be beneficial for the reproducibility and stability of the fabricated biosensor. Also, the biorecognition and amplification efficiency would be easily influenced by the electrode surface. In this context, the advance of homogenous or immobilization-free electrochemical biosensor could address the above issues to some extent in terms of operational simplicity and improved recognition or amplification efficiency.[11-14] However, the homogenous biosensor is usually operated by virtue of various nucleases, which increases the risk of false-positive signal output toward target detection. Also, the detection mechanism mostly relies on the diffusion or aggregation difference of electroactive labels before and after target-triggered nuclease operation, which might be more easily interfered by the complex sample matrix. Moreover, the lack of solid connection between signal reporter unit and electrode surface would be often plagued with the reduced detection reliability and reproducibility toward analytes. Thus, it has been emerged as a great challenge for the electrochemical biosensor fabrication that can display the striking detection sensitivity and specificity but not at the expense of simplicity, reliability and reproducibility. The biphasic operation mode with the

reliable working ability for both homogenous solution and heterogenous inteface would be conceived to offer a promising avenue to address the above issues.

Recently, the proximity-dependent immunoassays or aptasensors have been well developed for the simple-to-use and sensitive protein assays.[15-18] The key operation for these biosensors relies on simultaneous recognition of a target protein by a pair of affinity probes, which induces the oligonucleotide tails of the bound probes into close proximity for the promotion of ligation or hybridization.[19,20] Inspired by the concept of proximity-dependent immunosensor or aptasensor, herein, the dynamic DNA assembly-programmed surface hybridization effect was proposed for the development of single-step, reusable and enzyme-free amplified electrochemical nucleic acid biosensor. The dynamic DNA assembly strategies, most of which are driven by toehold-mediated strand displacement reaction (TSDR), have been widely applied for the fabrication of DNA nanostructures and biosensors.[21-26] In current study, three diverse dynamic DNA assembly strategies including DNA-fueled target recycling, catalytic hairpin DNA assembly (CHA) and hybridization chain reaction (HCR) were flexibly harnessed to convey the homogenous recognition and amplification events into various DNA scaffolds, which simultaneously created the proximate DNA motifs with their local concentration increased substantially in contrast to the isolated DNA motif for the successive proximity-based surface hybridization. The proposed dynamic DNA assembly-programmed surface hybridization strategy shows the following distinctive advantages. Firstly, it entirely inherits the inherent advantages of dynamic DNA assembly strategies including enzyme-free signal amplification, simplicity in sequence design and operational flexibility. Secondly, the homogenous operation for dynamic DNA assembly would be beneficial for the bio-recognition and amplification efficiency compared with the available heterogenous electrochemical

biosensors. Thirdly, autonomous execution of proximity-based surface hybridization makes it possible to realize single-step detection and minimize the operational difficulty.

Experimental section

Materials and chemicals. 6-Mercaptohexanol (MCH) and tris(2-carboxyethyl)phosphine (TCEP) were purchased from Sigma-Aldrich (St. Louis, MO, USA). Fetal calf serum was obtained from Sangon Biotech. Co., Ltd. (Shanghai, China). The HPLC-purified oligonucleotide sequences are purchased from Sangon Biotech. Co., Ltd. (Shanghai, China) and listed in Table S-1 to S-3. All other reagents were of analytical grade without further purification.

DNA immobilization. The electrode pretreatment was according to the previous procedures.[27] The pretreated gold electrode was immersed in a solution containing 1 μM thiolated oligonuleotide in 10 mM PBS buffer (0.2 M NaCl, 10mM TCEP, pH 7.4) for 12 h at room temperature. Afterward, the electrode was immersed into 1 mM MCH for 20 min to remove the nonspecific DNA adsorption.

DNA-fueled target recycling-programmed surface hybridization. The mixture of 1 μM protector DNA strand (PS), 1 μM assistant DNA strand (AS), and 1 μM template DNA strand (TS) in 10 mM PBS buffer (pH 7.4, 0.2 M NaCl) was heated to 90 ^{o}C for 10 min and then allowed to cool down to room temperature for at least 2 h to form the three-strand DNA duplex. The thiolated oligonucleotide immobilized electrode was incubated into 50 μL 10 mM PBS buffer (pH 7.4, 0.2 M NaCl) containing 0.1 μM above three-strand DNA duplex, 0.12 μM fuel DNA strand (FS) and various concentrations of target DNA (TD1) at 45 ^{o}C for 2 h. For hepatits B virus (HBV) DNA detection, 50 nM hairpin DNA transducer was added to the above three-strand DNA duplex mixture.

Catalytic hairpin DNA assembly (CHA)-programmed surface hybridization. The thiolated oligonucleotide immobilized electrode was

incubated into 50 μL 10 mM PBS buffer (pH 7.4, 0.2 M NaCl) containing 0.1 μM hairpin-like DNA-1 (HP1), 0.1 μM hairpin-like DNA-2 (HP2) and various concentrations of target DNA (TD2) at 45 °C for 2 h.

Hybridization chain reaction (HCR)-programmed surface hybridization. The thiolated oligonucleotide immobilized electrode was incubated into 50 μL 10 mM Tris-HCl (pH 7.4, 0.3 M NaCl, 1 mM $MgCl_2$) containing 0.1 μM hairpin-like DNA3 (HP3), 0.1 μM hairpin-like DNA4 (HP4) and various concentrations of target DNA (TD3) at 45 °C for 2 h.

Polyacrylamide gel electrophoresis. The dynamic DNA assembly products were analyzed by 17.5% polyacrylamide gel electrophoresis (PAGE) operated in 1×TAE buffer at 180 V for 3 min and then 135V for 90 min, followed by staining in ethidium bromide (EB) dye solution. The gels were scanned using the FR-980A gel image analysis system (Shanghai, China).

Electrochemical characterization. The electrochemical experiments were performed with a CHI 660D electrochemical workstation (CH Instruments, Shanghai, China). For DNA-fueled target recycling or CHA-programmed surface hybridization, the cyclic voltammetry (CV) and differential pulse voltammetry (DPV) were obtained in 10 mM PBS solution (pH 7.4, 0.2 M KNO_3). For HCR-programmed surface hybridization, the CV and square wave voltammetry (SWV) experiments were conducted in 20 mM Tris-HCl buffer (pH 7.4, 0.1 M NaCl).

RESULTS AND DISCUSSIONS

Principle of DNA-fueled target recycling-programmed surface hybridization. Herein, the DNA-fueled target recycling strategy was firstly used as a model for dynamic DNA assembly to program surface hybridization for single-step, enzyme-free, and amplified electrochemical nucleic acid detection, which was schematically

illustrated in Figure 1A. The DNA-fueled target recycling is autonomously operated by two cascaded toehold-mediated strand displacement amplification reactions (TSDR)[28-30]. The three-strand DNA duplex is firstly prepared by annealing the mixture of the template DNA strand (TS), assistant DNA strand (AS) and protector DNA strand (PS). The TS strand in the three-strand DNA duplex is engineered with a protruding 3′-ferrocene-labeled tail sequence that is complementary to the surface-tethered strand with a predesigned low melting temperature (Tm<37 ^{o}C). Also, the fuel DNA strand (FS) possesses the same tail sequence with TS at 3′-terminus. The target DNA (TD1) can hybridize with the first toehold region at the 5′-terminus of the TS and displace PS through the first TSDR. The displacement of PS by TD1 leads to the exposure of the initially blocked second toehold region in the middle of the TS, which subsequently hybridizes with the FS and triggers the second TSDR, resulting in the displacement of both TD1 and AS by the FS. The released TD1 would trigger the successive cascaded TSDR process, leading to the association of plenty of FS with TS. The tail sequences at both the 3′-terminus of TS and FS are thus brought into close proximity with their local concentration increased substantially to allow the pair of tail sequences to hybridize together with the surface-tethered DNA strands. Then the ferrocene labels of the tail sequence are drawn close to the electrode surface, producing a readily detectable redox current. In the absence of TD1, the TS and FS could not be initiated for the association together. Then, the tail sequence whether in the TS or FS does not autonomously associate with the surface-tethered strand because the complementary fragment is too short to promote effective annealing. Thus, the nucleic acid could be readily analyzed by current DNA-fueled target recycling-programmed surface hybridization. The CHA or HCR-programmed surface hybridization strategies would be discussed later in this work.

Electrochemical characterization of DNA-fueled target recycling-programmed surface hybridization. The Figure 1B shows the corresponding cyclic voltammetric (CV) responses in the presence and absence of TD1. A well-defined redox peak of ferrocene with the anodic and cathodic potential located at 308 mV and 202 mV, respectively, was obtained in the presence of TD1 (curve b in Figure 1B). Almost no evident electrochemical response could be observed in the absence of target DNA (curve a in Figure 1B). The CV peak current increased in linear correlation to the scan rates, featuring a typical surface-controlled electrochemical process (Figure S-1). The DPV responses were in well accordance with the results of CV (Figure 1C). In order to further verify that the electrochemical response was indeed aroused by the close proximity of two tail sequences at both the 3'-terminus of TS and FS after DNA-fueled target recycling, we attempted to explore the electrochemical responses by separately changing the tail sequence of TS or FS. Both the TS-2 and FS-2 are designed with the alternative polyT tail sequences at the 3'-terminus, which are not complementary with the surface-tethered strand. It could be seen from Figure 1D that, when the TS-2 or FS-2 was separately used as the substitute of TS or FS, no evident electrochemical responses were obtained after DNA-fueled target recycling operation. In these cases, only one tail sequence from TS or FS could be complementary with the surface-tethered strand after DNA-fueled target recycling process, which could not support the efficient association with the surface-tethered strands. Furthermore, when the TS-3 or FS-3 was individually employed for the substitute, the difference of which from TS or FS was that the ferrocene label was removed, respectively, approximate half of the electrochemical response could be only achieved, which strongly verified the proximity-based surface hybridization principle programmed by DNA-fueled target recycling. The DNA-fueled target recycling process was also verified by gel electrophoresis images (Figure 1E). It could be seen that a bright

band with obviously decreased migration shift was observed (Lane 6), indicating the formation of three-strand DNA duplex by the strands of TS, PS and AS. In the presence of TD1 and FS strand, a new band could be obtained (Lane 7), which could be attributed to the triggered assembly hybrids between TS and FS by TD1. Also, in the absence of TD1, such new band could not appear (Lane 8), verifying the DNA-fueled target recycling process for the association of TS and FS strands.

<<Herein For Figure 1>>

The electrode modification and biosensor fabrication process was further verified by electrochemical impedance spectroscopy (EIS) and CV characterization in $Fe(CN)_6^{3-/4-}$ solution (Figure S-2). The charge transfer resistance (Rct) increased continually during the biosensor fabrication process (Figure S-2A). Also, the redox peak current of $Fe(CN)_6^{3-/4-}$ decreased and the peak to peak potential separation increased following each step of the biosensor fabrication process (Figure S-2B). The EIS and CV results could consistently provide beneficial supports for the proximity-based surface hybridization programmed by DNA-fueled target recycling.

Optimization of experimental conditions. The numbers of hybridized base pairs between the surface-tethered strand and the tail sequence of TS or FS strand were firstly optimized (Figure 2A). The hybridized base number of 8 could achieve the better signal to background (S/B) ratio than that at number of 6 and 10. The less hybridized base number of 6 would not facilitate proximity-based surface hybridization programmed by DNA-fueled target recycling. More hybridized base number of 10 would induce a relatively increased background response. The immobilization concentration for surface-tethered oligonucleotide was also optimized (Figure 2B). The best electrochemical response could be obtained at the immobilization concentration of 1 μM based on the

obtained ΔI value (ΔI=I-I_0, the I and I_0 represents the electrochemical response in the presence of or not target DNA, respectively). The reaction temperature for the DNA assay was also investigated (Figure 2C). The background signal decreased with the reaction temperature, indicating that increased temperature weakened the possible recognition between the sole tail sequence of TS or FS and the surface-tethered strand. The response signal toward target DNA increased firstly and then decreased with the investigated rection temperature, which might be explained that the initially elevated temperature could accelerate the target recognition and the following DNA-fueled target recycling process for the generation of duplex DNA. The further elevated temperature would be not beneficial for the stability of the hybrids between two tail sequences of generated duplex DNA and surface-tethered strand. The optimized electrochemical response could be determined at 45 ^{o}C. It should be noted that the temperature effect on the electrochemical response might be adjusted to some extent by moderately adjusting the incubation time and the hybridized base numbers between the tail sequence of TS or FS and surface-tethered strand. The time response for the DNA-fueled target recycling-programmed surface hybridization process was also electrochemically monitored (Figure 2D). The background signal was only very slightly increased with the studied incubation time. The electrochemical response increased evidently with time at all three investigated target DNA concentrations. The electrochemical intensity almost reached the saturation value at 120 min when using a 1 nM target DNA. In the following experiment, the reaction time of 120 min was recommended for performance determination of the DNA biosensor.

<<Herein For Figure 2>>

Detection performance of DNA-fueled target recycling-programmed

surface hybridization strategy. Under the optimized experimental conditions, the detection performance of the fabricated electrochemical DNA sensor was investigated by using a series of different concentrations of target DNA ranged from 0 to 10 nM. As shown in Figure 3A, the dynamically increased DPV peak current with increasing target DNA concentration indicated that the DNA-fueled target recycling-programmed surface hybridization process was highly dependent on the concentration of target DNA. A good linear relationship between the electrochemical intensity and the logarithm value of target DNA concentration ranged from 0.5 fM to 1 nM could be obtained (Figure 3B). The regression equation was Y = 170.6 + 10.6 logX (Y and X represented the DPV peak current and target DNA concentration, respectively; unit of X was M) with the correlation coefficient of 0.9948. The detection limit, which was defined as 3 times the standard deviation of the background, was about 0.29 fM, which was superior or comparable with that of many reported electrochemical nucleic acid biosensors (Table S-4). Also, the relative standard deviations (RSDs) toward three different target DNA concentrations of 1 fM, 1 pM and 1 nM were obtained as 7.6%, 4.9% and 5.8%, respectively, based on six repetitive measurements, indicating a good reproducibility of our proposed strategy for target DNA detection. The specificity of the developed DNA sensing system was further investigated (Figure 3C). The electrochemical response toward single-base mismatched DNA (1MT) was about 25.6% of that for perfect target DNA. Three-bases mismatched DNA (3MT) showed only slightly increased electrochemical response compared with that for the blank solution. The developed biosensor should be readily regenerated since only a surface-tethered oligonucleotide monolayer with no preferred conformation is involved for sensor interface fabrication. It was found from Figure 3D that the proposed electrochemical nucleic acid biosensor could be regenerated over six times without significant signal loss via washing with 1 M NaOH for 10 min at 60 ^{o}C. Furthermore, the versatile sensing platform could be designed for the detection of virtually any DNA sequences by introducing an additional hairpin transducer (Figure

S-3A). This was exemplified with the detection of a hepatitis B virus (HBV) DNA fragment. A detection limit toward HBV DNA in the buffer system could be estimated as about 0.83 fM (Figure S-3B and C). Also, the electrochemical detection toward the spiked HBV DNA in the diluted healthy human serum sample was conducted (Figure S-3D and E). A detection limit of about 3.6 fM toward HBV DNA in the diluted human serum could be achieved, indicating the potentiality of the developed sensing platform for DNA detection in real biological samples.

<<Herein For Figure 3>>

Catalytic hairpin assembly-programmed surface hybridization. The dynamic DNA assembly-programmed surface hybridization was further demonstrated by using the catalytic hairpin assembly (CHA) technique, which could be considered as another typical enzyme-free target recycling strategy.[31,32] The fabrication principle is schematically illustrated in Figure S-4A. Both the hairpin-like DNAs (HP1 and HP2) contain the ferocene-labeled tail sequences at 3'-terminus, which are complementary to the surface-tethered DNA strands. Similar with the above DNA-fueled target recycling-programmed surface hybridization, the individual HP1 or HP2 could not associate with the surface-tethered strands. In the presence of target DNA (TD2), it could hybridize with and open the HP1 by means of a TSDR. The opened HP1 could further hybridize with the HP2 based on the TSDR again, accompanied with the release of target DNA to further propagate the assembly of HP1 and HP2. The formed HP1-HP2 hybrids after CHA bring the tail sequences at both 3'-terminus of HP1 and HP2 into close proximity to allow them to hybridize together with the surface-tethered DNA strands, resulting into the electrochemical response toward target DNA. The electrochemical responses toward different concentrations of target DNA were shown in Figure S-4B and C. The detection limit toward target DNA was estimated to be about 1.12 fM, which was higher than

that by DNA-fueled target recycling-programmed surface hybridization strategy. The weaken detection performance for CHA might be attributed to the relatively high background signal owing to the possible nonspecific reaction between two hairpin substrates.

Hybridization chain reaction-programmed surface hybridization. Hybridization chain reaction (HCR) could be regarded as another effective dynamic DNA assembly technique for post-amplification toward the biorecognition events.[24,33-35] Its validity to program surface hybridization for single-step and amplified biosensor fabrication is schematically illustrated in Figure 4A. Two hairpin-like DNAs (HP3 and HP4) are designed and the HP4 contains the methylene blue (MB)-labled tail sequence at 5'-terminus, which is complementary to the surface-tethered DNA strand. Again, HP4 itself could not associate with the surface-tethered strand. In the presence of target DNA (TD3), the alternate assembly between HP3 and HP4 by the sequential TSDRs leads to the formation of linear DNA concatamer, which accordingly brings the dangling tail sequence of HP4 into close proximity to endow the association together with the surface-tethered DNA strands for the electrochemical response toward target. The CV and square wave voltammetric (SWV) responses are shown in Figure 4B and C. A well-defined redox peak of MB with the anodic and cathodic potential located at -238 mV and -265mV, respectively, was only obtained in the presence of TD3 (curve b in Figure 4B). Also, the very well linear plots of anodic or cathodic peak currents with the scan rates verified that the MB has been confined on the electrode surface (Figure S-5). The SWV responses were in well accordance with the results of CV (Figure 4C). The target-triggered HCR process was also monitored by gel electrophoresis (Figure 4D). In the absence of TD3, only the bands related to the HP3 and HP4 could be observed (Lane 1). In the presence of TD3 (Lanes 2 to 5), the new bands with the slower migration rates could be observed, which could be attributed to the HCR products

between HP3 and HP4. Also, the average molecular weight of the product was inversely related to the amount of target, which was consistent with previous study.[36] The dynamic assembly process for target-triggered HCR could be also easily monitored by current proximity-based surface hybridization strategy (Figure 4E). At a high concentration of TD3 (1 nM), the electrochemical response increased rapidly and almost reached the plateau value after 2 h, indicating the rapid depletion of hairpin-like assembly unit. The electrochemical response increased slowly at the low concentration of target DNA. Especially for 1 fM TD3, the continually and sluggish electrochemical response increase could be observed during the whole monitoring process. The hybridized base number between the tail sequence of HP4 and the surface-tethered oligonucleotide was also optimized (Figure S-6). Similar with the DNA-fueled target recycling-programmed surface hybridization, the hybridized base number of 8 could also achieve the better S/B ratio than that at number of 6 and 10.

<<Herein For Figure 4>>

The detection performance of the HCR-programmed surface hybridization strategy was also investigated by using different concentrations of target DNA. The electrochemical intensity increased continually with the increase of TD3 concentration from 0 to 1 nM (Figure 5A). Figure 5B shows the calibration curve between the electrochemical intensity and the logarithm of the TD3 concentration ranging from 0.05 fM to 1 nM. A very low detection limit of 50 aM could be achieved, which was evidently lower than that by DNA-fueled target recycling and CHA. It might be tentatively explained that the electrochemical response would be more easily achieved at a relatively low concentration of target DNA owing to the target-triggered formation of DNA concatamer for the promotion of proximity-based surface hybridization. The electrochemical responses of the fabricated

biosensor toward 1MT and 2MT were about 28.2% and 18.5% of that for the perfect target DNA at the same concentration, respectively, indicating also a good performance to discriminate the perfect target from the base mismatched targets (Figure 5C). The electrochemical intensity increased also continually with the increase of the spiked target DNA concentration in the diluted fetal bovine serum (Figure 5D), verifying the detection feasibility of the fabricated biosensor in the relatively complex sample matrix. Also, the fabricated biosensor could be regenerated over six times via washing with 1 M NaOH for 10 min at 60 ^{o}C (Figure S-7). It seems that the HCR-programmed surface hybridization strategy shows a more favorable prospect for the point-of-care applications owing to its easier to operate, cost-effective and high sensititivty.

<<Herein For Figure 5>>

CONCLUSIONS

In summary, a versatile and unique dynamic DNA assembly-programmed surface hybridization strategy was proposed for the development of single-step, reusable and enzyme-free amplified electrochemical biosensor. Three dynamic DNA assembly strategies including DNA-fueled target recycling, CHA and HCR were flexibly engineered to create the proximate DNA motifs for the autonomous execution of proximity-based surface hybridization. The current biosensor architecture presented considerable advantages over the traditional nucleic acid-related biosensors, particularly in terms of assay simplicity, low cost and high sensitivity. Also, the reliable working ability for both homogenous solution and heterogenous interface endows the target detection with a robust reliability and reproducibility. Furthermore, it would be easily extended for the detection of a broad spectrum of targets owing to the growing trend for the detection universality of dynamic DNA assembly strategies. Thus, it holds great

potential for the development of sensitive biosensing platform for the applications in bioanalysis, disease diagnostics, and clinical biomedicine.

AUTHOR INFORMATION

Corresponding Author

* Tel.&Fax. 86-532-84022681. E-mail address: sliu@qust.edu.cn

Notes

The authors declare no competing financial interest.

ACKNOWLEDGEMENTS

This work was funded by the National Natural Science Foundation of China (No. 21475072), the Natural Science Foundation of Shandong Province of China (Nos. ZR2015JL007, ZR2014BM019) and the Key Research and Development Program of Shandong Province of China (2016GSF201208).

ASSOCIATED CONTENT

Supporting Information. The synthesized DNA sequences (Table S-1 to S-3). The additional characterizations toward DNA-fueled target recycling (Figure S-1 to S-3), CHA (Figure S-4) and HCR-programmed surface hybridization (Figure S-5 to S-7). This information is available free of charge via the Internet at http://pubs.acs.org/

REFERENCES

(1) Das, J.; Ivanov, I.; Montermini, L.; Rak, J.; Sargent, E. H.; Kelley, S. O. *Nat. Chem.* **2015**, *7*, 569-575.

(2) Wang, F.; Lu, C. H.; Liu, X.; Freage, L.; Willner, I. *Anal. Chem.* **2014**, *86*, 1614-1621.

(3) Venkatesan, B. M.; Bashir, R. *Nat. Nanotech.* **2011**, *6*, 615-624.

(4) Wang, F.; Lu, C. H.; Willner, I. *Chem. Rev.* **2014**, *114*, 2881-2941.

(5) Privett, B. J.; Shin, J. H.; Schoenfisch, M. H. *Anal. Chem.* **2008**, *80*, 4499-4517.

(6) Xuan, F.; Fan, T. W.; Hsing, I. M. *ACS Nano* **2015**, *9*, 5027-5033.

(7) Xiao, Y.; Lai, R. Y.; Plaxco, K. W. *Nat. Protoc.* **2007**, *2*, 2875-2880.

(8) Zhao, Y.; Chen, F.; Li, Q.; Wang, L.; Fan, C. *Chem. Rev.* **2015**, *115*, 12491-12545.

(9) Craw, P.; Balachandran, W. *Lab Chip* **2012**, *12*, 2469-2486.

(10) Duan, R.; Lou, X.; Xia, F. *Chem. Soc. Rev.* **2016**, *45*, 1738-1749.

(11) Xuan, F.; Luo, X.; Hsing, I. M. *Anal. Chem.* **2012**, *84*, 5216-5220.

(12) Nie, J.; Zhang, D. W.; Zhang, F. T.; Yuan, F.; Zhou, Y. L.; Zhang, X. X. *Chem. Commun.* **2014**, *50*, 6211-6213.

(13) Tan, Y.; Wei, X.; Zhao, M.; Qiu, B.; Guo, L.; Lin, Z.; Yang, H. H. *Anal. Chem.* **2015**, *87*, 9204-9208.

(14) Zhuang, J.; Tang, D.; Lai, W.; Chen, G.; Yang, H. *Anal. Chem.* **2014**, *86*, 8400-8407.

(15) Hu, J.; Wang, T.; Kim, J.; Shannon, C.; Easley, C. J. *J. Am. Chem. Soc.* **2012**, *134*, 7066-7072.

(16) Zhang, Y. L.; Huang, Y.; Jiang, J. H.; Shen, G. L.; Yu, R. Q. *J. Am. Chem. Soc.* **2007**, *129*, 15448-15449.

(17) Li, C.; Li, X.; Wei, L.; Liu, M.; Chen, Y.; Li, G. *Chem. Sci.* **2015**, *6*, 4311-4317.

(18) Fredriksson, S.; Gullberg, M.; Jarvius, J.; Olsson, C.; Pietras, K.; Gústafsdóttir, S. M.; Ostman, A.; Landegren, U. *Nat. Biotechnol.* **2002**, *20*, 473-477.

(19) Giusto, D. A. D.; Wlassoff, W. A.; Gooding, J. J.; Messerle, B. A.; King, G. C. *Nucl. Acids Res.* **2005**, *33*, e64.

(20) Zhang, H.; Li, F.; Dever, B.; Wang, C.; Li, X. F.; Le, X. C. *Angew. Chem. Int. Ed.* **2013**, *52*, 10698-10705.

(21) Jung, C.; Ellington, A. D. *Acc. Chem. Res.* **2014**, *47*, 1825-1835.

(22) Qian, L.; Winfree, E. *Science* **2011**, *332*, 1196-1201.

(23) Zhang, D. Y.; Seelig, G. *Nat. Chem.* **2011**, *3*, 103-113.

(24) Dirks, R. M.; Pierce, N. A. *Proc. Natl. Acad. Sci. USA* **2004**, *101*, 15275-15278.

(25) Li, F.; Zhang, H.; Wang, Z.; Li, X.; Li, X. F.; Le, X. C. *J. Am. Chem. Soc.* **2013**, *135*, 2443-2446.

(26) Yang, X.; Tang, Y.; Traynor, S. M.; Li, F. *J. Am. Chem. Soc.* **2016**, *138*, 14076-14082.

(27) Liu, S.; Wang, C.; Zhang, C.; Wang, Y.; Tang, B. *Anal.Chem.* **2013**, *85*, 2282-2288.

(28) Zhang, D. Y.; Turberfield, A. J.; Yurke, B.; Winfree, E. *Science* **2007**, *318*, 1121-1125.

(29) Shi, K.; Dou, B.; Yang, C.; Chai, Y.; Yuan, R.; Xiang, Y. *Anal. Chem.* **2015**, *87*, 8578-8583.

(30) Lv, Y.; Cui, L.; Peng, R.; Zhao, Z.; Qiu, L.; Chen, H.; Jin, C.; Zhang, X. B.; Tan, W. *Anal. Chem.* **2015**, 87, 11714-11720.

(31) Yin, P.; Choi, H. M. T.; Calvert, C. R.; Pierce, N. A. *Nature* **2008**, *451*, 318-322.

(32) Li, B.; Ellington, A. D.; Chen, X. *Nucl. Acids Res.* **2011**, *39*, e110;

(33) Shimron, S.; Wang, F.; Orbach, R.; Willner, I. *Anal. Chem.* **2012**, *84*, 1042-1048.

(34) Xuan, F.; Hsing, I. M. *J. Am. Chem. Soc.* **2014**, *136*, 9810-9813.

(35) Wang, F.; Elbaz, J.; Orbach, R.; Magen, N.; Willner, I. *J. Am. Chem. Soc.* **2011**, *133*, 17149-17151.

(36) Chen, Y.; Xu, J.; Su, J.; Xiang, Y.; Yuan, R.; Chai, Y. *Anal. Chem.* **2012**, *84*, 7750-7755.

Figure Captions

Figure 1. (A) Schematic illustration of DNA-fueled target recycling-programmed surface hybridization strategy for nucleic acid biosensor fabrication. (B) and (C) show the CV and DPV responses for the fabricated biosensor toward blank (a) and 1 nM target DNA (TD1) (b) in 10 mM PBS (pH 7.4, 0.2 M KNO_3), respectively. (D) The bar chart of the electrochemical response toward blank and 1 nM TD1 when the TS and FS strands were replaced by their respective substitutes. The tail sequences in TS-2 and FS-2 could not be complementary with the surface-tethered oligonucleotide. Both TS-3 and FS-3 contain no ferrocene label at the 3'-terminus. (E) Non-denaturing PAGE analysis: lane 1, 5 μM TS; lane 2, 10 μM AS; lane 3, 10 μM PS; lane 4, 10 μM TD1; lane 5, 5 μM FS; lane 6, 1 μM TS, 1 μM AS and 1 μM PS; lane 7, 0.1 μM three-strand duplex, 0.12 μM FS and 1 nM TD1; lane 8, 0.1 μM three-strand duplex and 0.12 μM FS.

Figure 2. (A) The optimization of the hybridized base numbers between surface-tethered oligonucleotide and tail sequence of TS or FS. (B) The immobilization concentration optimization for the surface-tethered oligonucleotide. Five different oligonucleotide concentrations including 0.1, 0.5, 1.0, 1.5 and 2.0 μM were studied. (C) The optimization of reaction temperature. The reaction temperatures from 25 ^{o}C to 55 ^{o}C were used for the electrochemical responses toward 1 nM TD1 (triangle) and blank solution (circle). (D) The time dependency of the electrochemical responses toward blank and three different TD1 concentrations (1 fM, 1 pM, and 1 nM).

Figure 3. (A) DPV responses corresponding to the analysis of different concentrations of TD1 ranged from 0 to 10 nM. (B) The linear relationship between the DPV peak current and the logarithm value of the TD1 concentration. Error bars represent standard deviations of measurements (n=3). (C) Selectivity tests of the fabricated DNA biosensor toward 10 nM of complementary target DNA (TD1), single-base mismatched DNA (1MT), three-bases mismatched DNA (3MT), non-complementary DNA (NC), and the absence of DNA (Blank). Error bars represent standard deviations of

measurements (n=3). (D) The regeneration experiments of the fabricated biosensor by DNA-fueled target recycling-programmed surface hybridization. The concentrations of target DNA was 10 nM. The regeneration experiments were conducted via washing with 1 M NaOH for 10 min at 60 ^{o}C.

Figure 4. (A) The schematic illustration for the HCR-programmed surface hybridization strategy. (B) and (C) shows the CV and SWV responses toward blank (a) and 1 nM TD3 (b) in the 20 mM Tris-HCl (pH 7.4, 0.1 M NaCl) buffer, respectively. (D) Non-denaturing PAGE analysis. Lanes 1 to 5 were obtained in the presence of 1 μM HP3 and 1 μM HP4 with the TD3 concentrations of 0, 5, 1, 0.1 and 0.01 μM, respectively. (E) The time dependency of the electrochemical responses toward blank and three different TD3 concentrations (1fM, 1 pM, and 1 nM).

Figure 5. (A) SWV responses corresponding to the analysis of different concentrations of TD3 ranged from 0 to 1 nM. (B) The calibration curve between the SWV peak current and the logarithm value of the TD3 concentration. Error bars represent standard deviations of measurements (n=3). (C) Bar chart of SWV peak currents obtained at 1 nM of complementary target DNA (TD3), single-base mismatched DNA (1MT), two-bases mismatched DNA (2MT), noncomplementary DNA (NC) and blank solution. The inset shows the corresponding SWV curves. (D) SWV responses obtained at different concentrations of TD3 spiked in 10% diluted fetal calf serum.

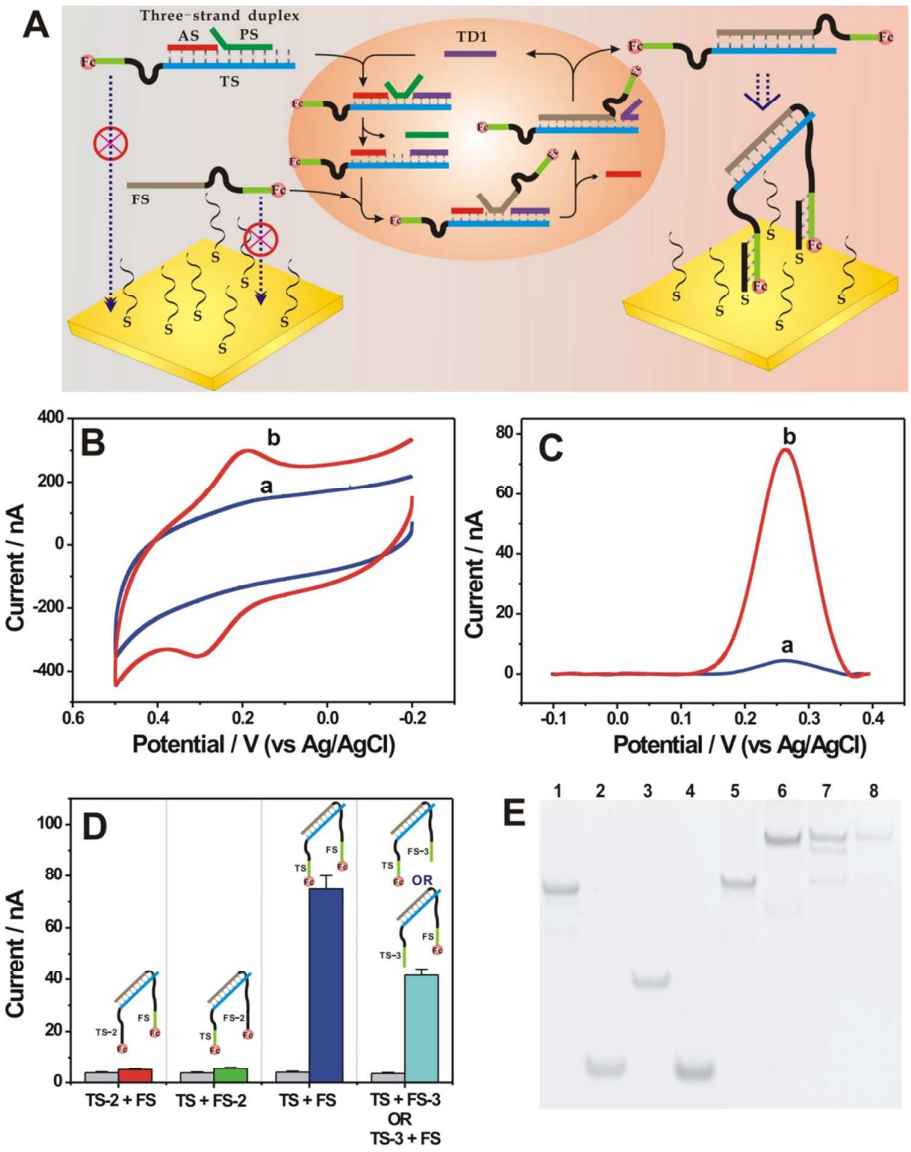
A
Three-strand duplex
AS
PS
TS
TD1
FS
Fc
S
B
b
a
Current / nA
Potential / V (vs Ag/AgCl)
C
b
a
Current / nA
Potential / V (vs Ag/AgCl)
D
Current / nA
TS-2 + FS
TS + FS-2
TS + FS
TS + FS-3
OR
TS-3 + FS
E
1 2 3 4 5 6 7 8

Figure 1

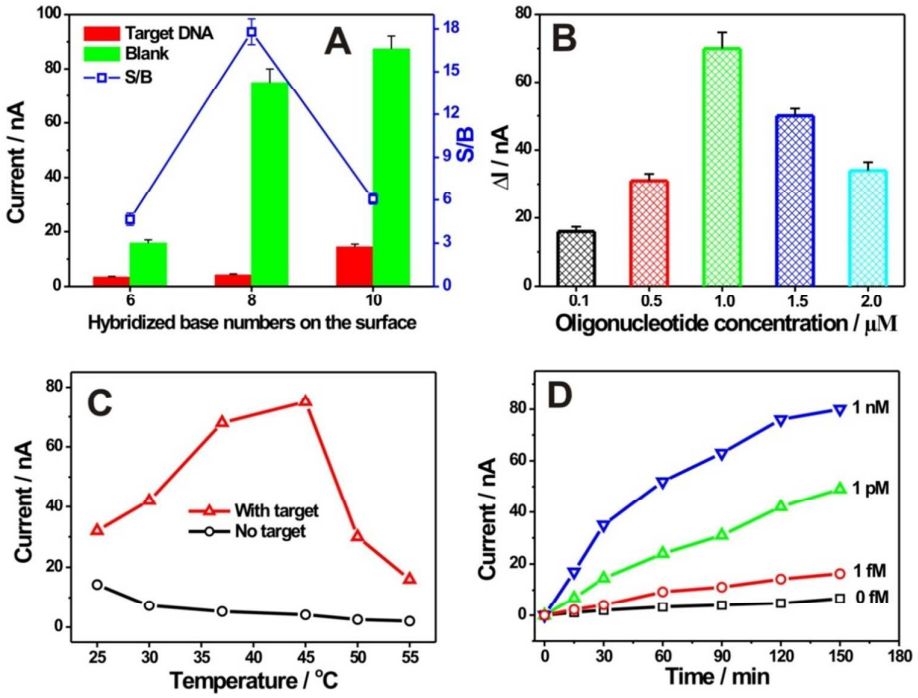
A
Target DNA
Blank
S/B
Current / nA
S/B
Hybridized base numbers on the surface
B
ΔI / nA
Oligonucleotide concentration / μM
C
With target
No target
Current / nA
Temperature / °C
D
1 nM
1 pM
1 fM
0 fM
Current / nA
Time / min

Figure 2

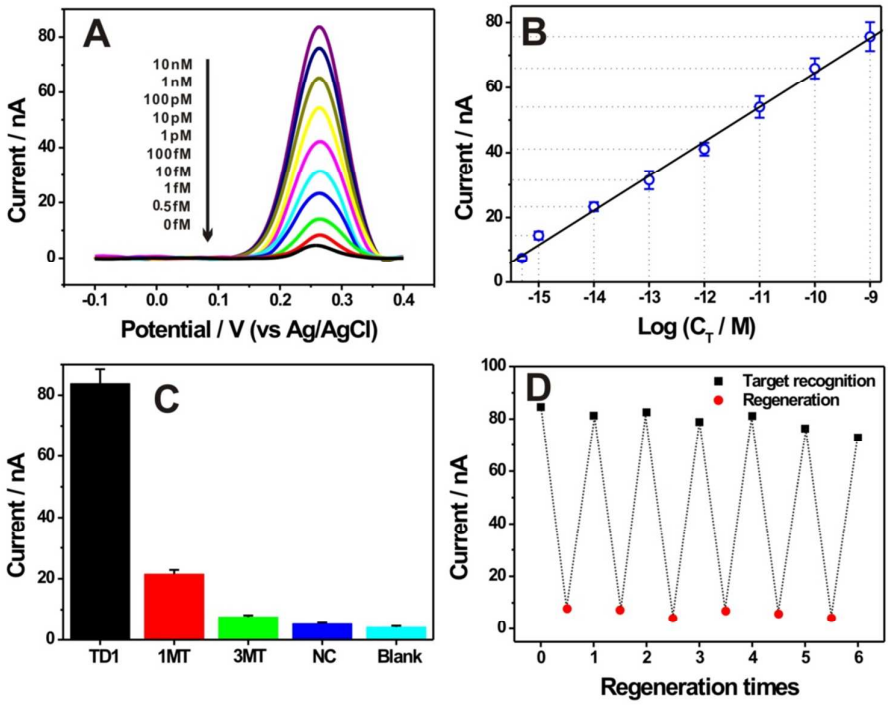
A
10nM
1nM
100pM
10pM
1pM
100fM
10fM
1fM
0.5fM
0fM
Current / nA
Potential / V (vs Ag/AgCl)
B
Current / nA
Log (C_T / M)
C
Current / nA
TD1
1MT
3MT
NC
Blank
D
Target recognition
Regeneration
Current / nA
Regeneration times

Figure 3

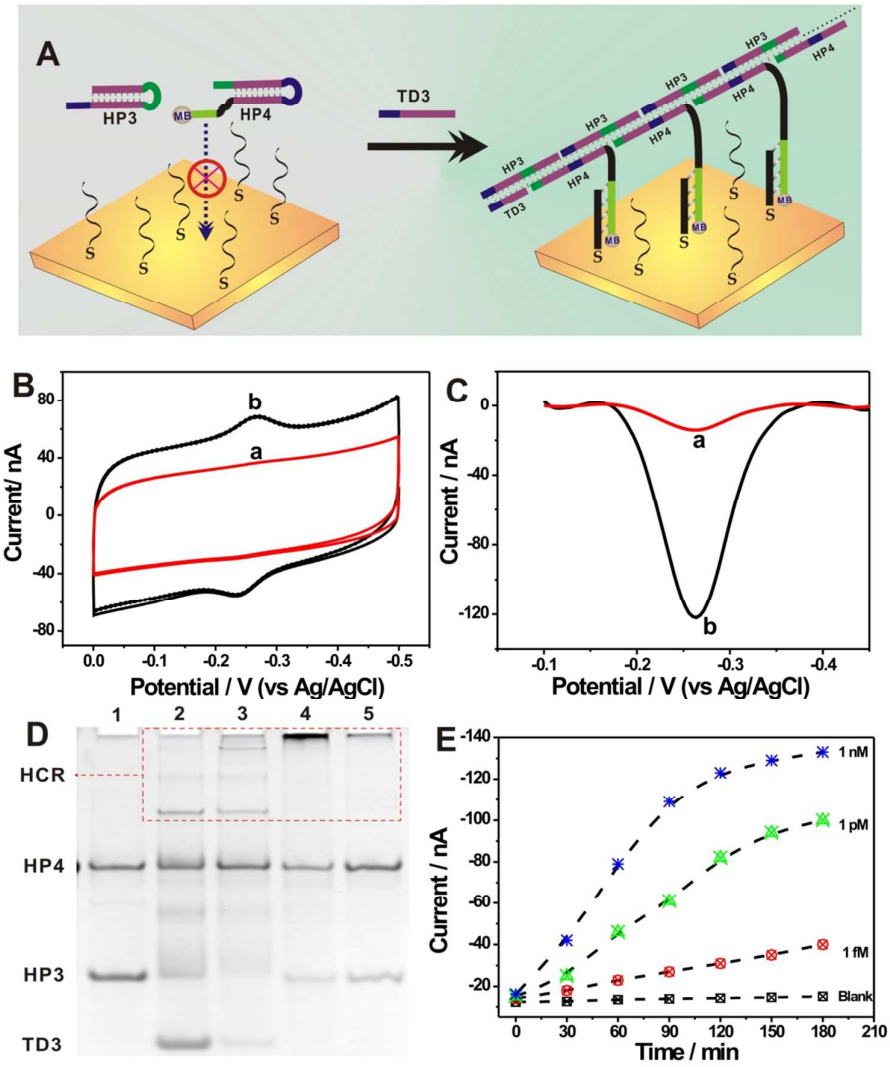
A
HP3
MB
HP4
TD3
S
B
Current/ nA
Potential / V (vs Ag/AgCl)
a
b
C
Current / nA
Potential / V (vs Ag/AgCl)
a
b
D
1
2
3
4
5
HCR
HP4
HP3
TD3
E
Current / nA
Time / min
1 nM
1 pM
1 fM
Blank

Figure 4

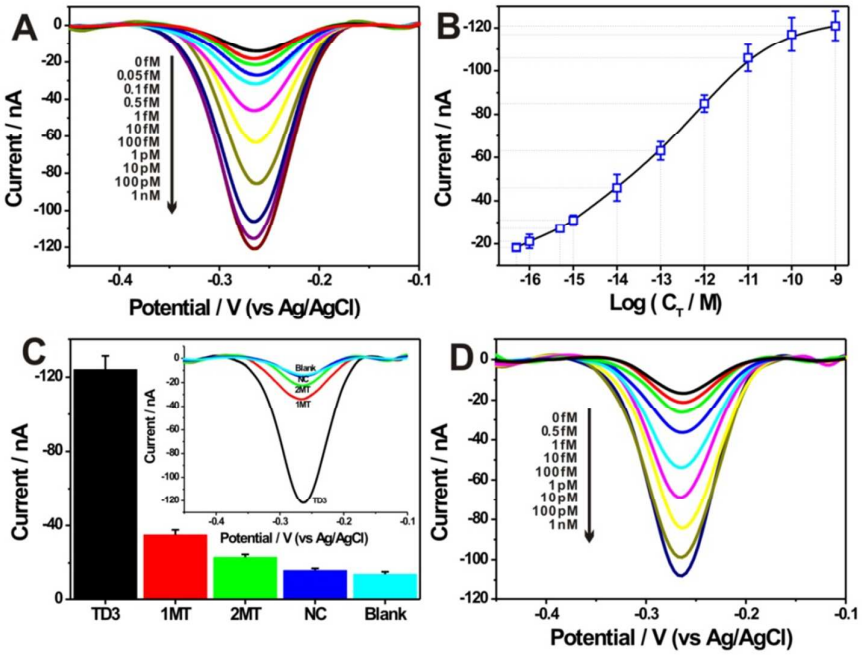
A
Current / nA
Potential / V (vs Ag/AgCl)
0 fM
0.05 fM
0.1 fM
0.5 fM
1 fM
10 fM
100 fM
1 pM
10 pM
100 pM
1 nM
B
Current / nA
Log (C_T / M)
C
Current / nA
TD3
1MT
2MT
NC
Blank
Potential / V (vs Ag/AgCl)
D
Current / nA
0 fM
0.5 fM
1 fM
10 fM
100 fM
1 pM
10 pM
100 pM
1 nM
Potential / V (vs Ag/AgCl)

Figure 5
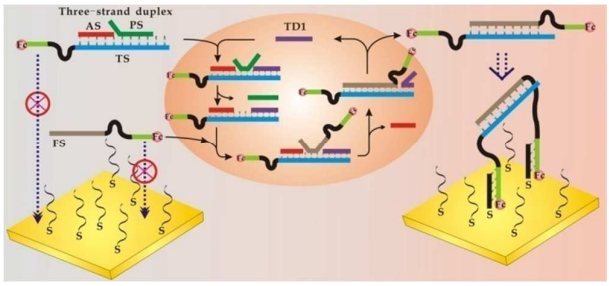
For TOC only